Journal of Solid State Chemistry **155,** 1–8 (2000)
doi:10.1006/jssc.2000.8874, available online at http://www.idealibrary.com on IDEAL®

Quantification of the Interlayer Charge Transfer, via Bond Valence Calculation, in 2D Misfit Compounds: The Case of $(Pb(Mn,Nb)_{0.5}S_{1.5})_{1.15}NbS_2$

C. Deudon,[1] A. Lafond, O. Leynaud, Y. Moëlo, and A. Meerschaut

Institut des Matériaux Jean Rouxel, UMR 6502 CNRS—Université de Nantes, Laboratoire de Chimie des Solides, 2, rue de la Houssinière, BP 32229, 44322 Nantes cedex 03, France

Received March 7, 2000; in revised form July 6, 2000; accepted July 17, 2000

DEDICATED TO PROFESSOR J. M. HONIG

The new layered misfit sulfide of the 1.5Q/1H homologue type, $(Pb(Mn,Nb)_{0.5}S_{1.5})_{1.15}NbS_2$, has been synthesized. Electron probe microanalysis gives the chemical formula $(Pb_{1.02}Mn_{0.33}Nb_{0.16}S_{1.50})_{1.15}NbS_2$, indicating Nb incorporation in the rock-salt-type part (Q layer). Its crystal structure has been solved through a superspace approach: orthorhombic symmetry, superspace group *Cm2m*(α00), cell parameters $a = 3.326(1)$, $b = 5.788(1)$, $c = 14.326(3)$ Å, q vector (0.5744(2),0,0); $R = 2.27\%$ for 688 reflections and 36 variables. Nb-for-Mn substitution in the central part of the Q layer is clearly proved. Bond valence calculation on this compound, compared to some other misfit compounds, makes it possible to evaluate the charge transfer that governs the stability of such composite materials. This calculation, which takes into account the modulation of Pb–S_H bondings at the Q/H interface through the superspace approach, shows that the transfer depends on the nature of cations in the Q layer. This leads to a formal oxidation state for Nb, within the H layer, varying between ~3 and 3.6. © 2000 Academic Press

Key Words: **sulfide; lead; manganese; niobium; structure determination; bond valence.**

INTRODUCTION

The composite structure of the misfit-layered chalcogenides $(MX)_{1+x}TX_2$ (where M = Sn, Pb, rare earth metals; T = Ti, V, Cr, Nb, Ta; X = S, Se; $1.08 < 1 + x < 1.28$) results from the alternate stacking of MX slabs (rock-salt-type layer, named Q) and TX_2 slabs (edge-sharing octahedra for T = Ti, V, Cr or edge-sharing trigonal prisms for T = Nb, Ta; layer named H) (1). The incommensurate character is due to the fact that the ratio of the a parameters of the two sublattices is not a rational number.

The question of stability for such misfit phases, against a mixture of pure binary compounds, has been already largely discussed in previous papers (2–5). According to recent results, it clearly appears that the stability of misfit layer compounds is always governed by a charge transfer mechanism (6). This electron transfer directly results from the chemical bonding, at the Q/H interface, between M atoms protruding outward from the Q layer (see Fig. 1a) and X_H atoms of the H layer. Thus the bond valence method which focused on M–X_H bonds, is a good tool for calculating the interlayer charge transfer between the two sublattices. So, to do this, the respective M–X_H distances must be determined precisely, which needs the use of the superspace approach to know the exact bond lengths for such a modulated structure. Results will be compared with similar data obtained on some other misfit compounds.

The compound studied belongs to the 1.5Q/1H homologue type (Fig. 1b), where the three-atom-thick Q layer alternates with the H layer. Such an homologue was first obtained with $(Pb_{1.0}Fe_{0.5}S_{1.5})_{1.15}NbS_2$ (7, 8), and $[(EuS)_{1.5}]_{1.15}NbS_2$ (9). In these two compounds, the charge transfer is clearly due to the presence of a trivalent cation in the central atomic plane of the Q layer. Obtaining another compound by substituting In^{3+} for Fe^{3+} ascertains the amount of the charge transfer. Since for Nb metallic misfit compounds the superconductivity is attached to a minimal charge transfer, as this was proposed for homologues with divalent M cations (8–11), syntheses were then performed with a divalent cation substituting for Fe^{3+} for a better chance of obtaining a superconductor. The Cd and Mn derivatives were thus prepared, but only the Mn batch showed single crystals suitable for a complete structure determination through a superspace approach.

SYNTHESES AND CHEMICAL ANALYSIS

Synthesis of $(Pb(Mn,Nb)_{0.5}S_{1.5})_{1.15}NbS_2$ has been made by a classical solid state chemistry route. The precursors

[1] To whom correspondence should be addressed. Fax: (33) 2 40 37 39 95. E-mail: Catherine. Deudon@cnrs-imn.fr.

0022-4596/00 $35.00

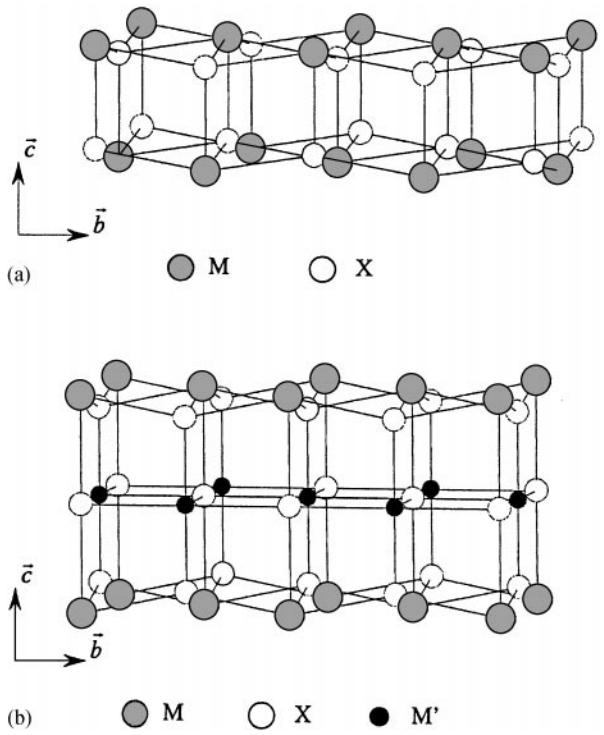

FIG. 1. The Q layer in the 2D misfit compounds viewed along (100). Homologues 1Q/1H $[(MX)]_{1+x}TX_2$ (a), and 1.5Q/1H $\{[(M, M')S]_{1.5}\}_{1+x}TS_2$ (b).

PbS, NbS_2, Mn, and S were weighted in the same ratio as for the Fe homologue (8) (i.e.,1.16:1:0.58:0.58, respectively), and loaded into a quartz tube sealed under primary vacuum. The mixture was progressively heated and maintained at 800°C for one week. The crystallized powder contained a small amount of MnS in excess. Few small crystals in a platelet shape of the new phase could be selected. Unfortunately, recrystallization with iodine did not yield larger crystals of the 1.5Q/1H phase, leading essentially to the growth of crystals of $[(Pb,Nb)S]_{1.14}NbS_2$. A lot of selected crystals were twinned.

Electron probe microanalysis was performed on the Pb/Mn/Nb misfit compound together with associated binary sulfides. Synthetic products were included in epoxy, then prepared as a polished section for a metallographic study. Two samples were considered, the first with the compound studied, the second without Pb in the starting product (in order to confirm the absence of any misfit phase in the pure Mn–Nb–S system). After examination under the metallographic microscope, selected synthetic crystals were analyzed with a CAMECA SX 50 microprobe (BRGM-CNRS-University common analytical service, Orléans). Operating conditions were as follows: voltage 20 kV, sample current 20 nA, counting time for each spot analysis 10 s, standards (element, emission line): PbS (Pb$M\alpha$), Mn metal (Mn$K\alpha$), Nb metal (Nb$L\alpha$), FeS_2 (S$K\alpha$). Table 1 presents the microanalyses, and Fig. 2 their projection in the (Pb, Mn)–Nb–S system. The following phases were detected:

— in the sample without Pb, MnS was associated with the classic intercalated compound $Mn_{0.25}NbS_2$;

— in the sample with Pb, PbS (galena) was associated with two misfit compounds of the 1Q/1H and 1.5Q/1H types.

The 1Q/1H misfit compound contains only a very low amount of Mn (< 0.4 wt.%). Its composition is very close to that already published (10), with significant substitution of Pb by Nb within the Q layer. In contrast, the 1.5Q/1H misfit compound contains Mn as a major constituent, and is similar to the corresponding misfit homologue with Pb, Fe, and Nb (7,8). Nevertheless, on the basis of the general formula $(PbM_{0.5}S_{1.5})_{1+x}NbS_2$ (M = transition metal), it clearly appears to have a Mn deficit, correlated to an excess

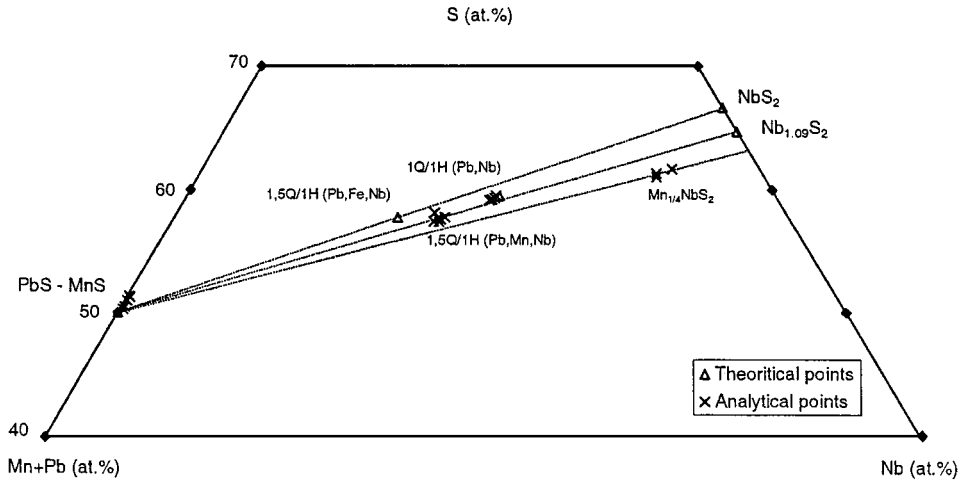

FIG. 2. Projection of the EPMA results in the (Pb, Mn)–Nb–S system.

TABLE 1
Electron Probe Microanalysis of the $(Pb(Mn, Nb)_{0.5}S_{1.5})_{1.15}NbS_2$ Compound and Associated Sulfides

		Wt.%					Atom ratios			
Phase	No.	Pb	Mn	Nb	S	Total	Pb	Mn	Nb	S Fixed
PbS	4	84.40	1.02	0.16	14.42	100.00	0.906	0.041	0.004	1
	5	84.98	0.91	0.15	14.27	100.31	0.921	0.037	0.004	1
	6	84.39	0.89	0.13	14.36	99.78	0.909	0.036	0.003	1
MnS	21	0.08	63.13	0.48	37.76	101.45	0.000	0.976	0.004	1
	23	0.15	63.39	0.48	37.58	101.60	0.001	0.984	0.004	1
1.5Q/1H	7	49.10	4.69	22.14	24.23	100.16	1.171	0.422	1.177	3.732
(Pb, Mn, Nb)	8	48.91	4.49	21.86	24.60	99.86	1.148	0.398	1.145	3.732
	9	47.95	4.37	21.94	23.93	98.18	1.157	0.398	1.181	3.732
	13	50.13	3.88	22.20	23.80	100.01	1.216	0.355	1.202	3.732
	14	48.85	4.08	22.80	24.36	100.10	1.158	0.365	1.206	3.732
	16	48.93	4.03	22.22	23.89	99.06	1.183	0.367	1.198	3.732
						Mean	**1.17**	**0.38**	**1.18**	**3.73**
1Q/1H	10	50.14	0.12	25.18	24.26	99.70	1.009	0.009	1.130	3.155
(Pb, Nb)	11	49.92	0.23	24.99	24.01	99.15	1.015	0.018	1.133	3.155
	12	50.25	0.33	24.91	24.03	99.52	1.021	0.025	1.129	3.155
	15	49.84	0.40	24.43	23.69	98.36	1.027	0.031	1.123	3.155
						Mean	**1.018**	**0.021**	**1.129**	**3.155**
$Mn_{1/4}NbS_2$	18	—	7.55	55.69	37.53	100.77	—	0.235	1.024	2
	19	—	7.77	56.48	37.72	101.97	—	0.240	1.034	2
	20	—	6.19	56.55	37.29	100.03	—	0.194	1.047	2
						Mean	**—**	**0.223**	**1.035**	**2**

of Nb (while Pb content agrees with that expected). This corresponds to an horizontal shift of the analyses (Fig. 2) relative to the Fe homologue, suggesting a selective substitution of Mn by Nb, with the structural formula $(Pb_{1.02}Mn_{0.33}Nb_{0.16}S_{1.5})_{1.15}NbS_2$.

For comparison, microprobe analysis of the 1.5Q/1H homologue synthesized with indium gives the structural formula $(Pb_{1.09}In_{0.56}Nb_{0.02}S_{1.50})_{1.15}NbS_2$, where the Nb "excess" is too small to be indicative of substitution with indium in the Q layer. In contrast the cadmium derivative corresponds to $(Pb_{0.98}Cd_{0.36}Nb_{0.15}S_{1.50})_{1.15}NbS_2$; similar to Mn, the use of a divalent metal inside the Q layer necessitates the partial incorporation of Nb, with the same substitution level of the central M cation.

STRUCTURE DETERMINATION OF $(Pb(Mn, Nb)_{0.5}S_{1.5})_{1.15}NbS_2$

General Approach

Structural determinations for such 2D incommensurate compounds can be made either through the composite approach or through the superspace approach (12–16). With the composite description, each subsystem has its own 3D space group and unit cell parameters. Then, the use of common reflections ($0kl$) makes it possible to refine the relative arrangement between both parts. In that way, modulation is not taken into account; i.e., one obtains the average structures for both parts, which does not give the relative atomic positions along the a axis, and the true interatomic distances cannot be determined between M and X_H atoms. Indeed, interaction between the two subsystems leads to mutual displacive modulations with the wave vector for one subsystem being dictated by the other subsystem; for instance the wave vector coordinates for the Q part are $(\alpha, 0, 0)$ where α is a_Q^*/a_H^*. The existence of such a modulation gives rise to satellite reflections in the diffraction pattern. Even if these satellite reflections were not recorded because of their too low intensities, the modulated structure can be determined because main reflections have contributions from both Q and H subsystems. In such an incommensurate composite structure, the atomic coordinates of the atom μ are expressed as

$$x_i^{\mu} = x_i^{\mu o} + n_i + u_i^{\mu}(\bar{x}_4), \qquad [1]$$

where $x_i^{\mu o}$ is the coordinate of the atom μ in the unit cell of the basic structure along the axis i ($i = 1, 2$, or 3 respectively for x, y, and z), n_i an integer representing the lattice translation and $u_i^{\mu}(\bar{x}_4)$ the modulation function. The argument $\bar{x}_4$ is the coordinate of the atom in the fourth direction of the

superspace. This coordinate depends on the value of the phase t of the modulation wave. This modulation function can be expanded in Fourier series often limited to the first order:

$$u_i^{\mu}(\bar{x}_4) = A_i^{\mu} \sin(2\pi\bar{x}_4) + B_i^{\mu} \cos(2\pi\bar{x}_4). \quad [2]$$

The distance between two neighboring atoms, in the same sublattice, is different in all unit cells of the basic structure and so takes an infinity of values. The superspace description allows a representation of all these different values as a continuous function of t. This periodic function shows all the interatomic distances that can be found in the whole crystal between two selected atoms. The description is more complex when the two atoms belong to different sublattices. However, it is possible to describe the whole basic structure in a superspace group, and hence, to calculate the interatomic distances M–X_H.

The whole structural determination procedure in a superspace group for a misfit layered compound with the 1.5Q/1H alternate sequence was already detailed in a previous study on $[(EuS)_{1.5}]_{1.15}NbS_2$ (9). The structural determination of $(Pb(Mn,Nb)_{0.5}S_{1.5})_{1.15}NbS_2$ is presented following this approach.

Structure Refinement

Single-crystal X-ray data collection was performed on a STOE-IPDS diffractometer (17), using Mo$K\alpha$ radiation ($\lambda = 0.71073$ Å) with an exposure time of 5 min. for each plate, for the restricted θ range $1.42^\circ < \theta < 25.76^\circ$. Experimental conditions are collected in Table 2.

Reflections were indexed in two subsets for an orthorhombic symmetry. The first consists of the main reflections from the H part and the satellite reflections indexed in a (3 + 1)-dimensional space. The second concerns the main reflections of the Q part. Intensities were corrected for Lorentz and polarization effects, and for absorption (analytic method using a Gaussian integration); then, the two subsets of reflections were merged in a unique set of $hklm$ reflections. The $0klm$ reflections are the $h_Qk_Ql_Q$ reflections of the Q part with $m = h_Q$. The $0kl0$ reflections, which belong to the two sublattices, are used to scale the intensities of the two sets of reflections. True satellite reflections are characterized with both h and m different from zero.

The superspace group, $Cm2m(\alpha00)$, was deduced from the space group of each 3D substructure: $Cm2m$ for the H part and $Cmmm$ for the Q part. All the recorded reflections satisfied the extinction condition of this superspace group except for the $4klm$ ones. This fact can be explained by a partial overlap between $4klm$ satellite reflections and $0kl(m + 7)$ main reflections because the wave vector component, $\alpha = a_Q^*/a_H^* = 0.5744$, is close to $4/7 = 0.5714$ ("semi-commensurate" approximation).

TABLE 2
Crystallographic Data, Experimental Details for $(Pb(Mn, Nb)_{0.5}S_{1.5})_{1.15}NbS_2$

Crystallographic data	
Structural formula	$Pb_{1.15}Mn_{0.45}Nb_{1.12}S_{3.73}$
Color	Black
Molar weight ($g\,mol^{-1}$)	487.18
Crystal system	Orthorhombic
Superspace group	$Cm2m(\alpha\,0\,0)$
Temperature (K)	293
Cell parameters	Calculated from 1158 reflections
a; b; c (Å)	3.326(1); 5.788(1); 14.326(3)
V (Å^3)	275.8(1)
q vector	(0.5744(2), 0, 0)
Z	2
Calc. density ($g\,cm^{-3}$)	5.865
Crystal shape	Platelet
Crystal size (mm^3)	$\sim 0.08 \times 0.16 \times 0.01$
Data collection	
Monochromator	Oriented graphite (002)
Radiation	Mo K–$L_{2,3}$ ($\lambda = 0.71073$ Å)
	H part / Q part
$hklm$ range	$-4 < h < 4$ / $h = 0$
	$-6 < k < 6$ / $-6 < k < 6$
	$-17 < l < 17$ / $-17 < l < 17$
	$-2 < m < 2$ / $-6 < m < 7$
$\sin(\theta)/\lambda$ range	0–0.613
Data reduction	
Absorption coefficient (cm^{-1})	396.1
Absorption correction	Gaussian method
T_{min}/T_{max}	0.06/0.45
Reflections used to scale the different subsets of reflections	1804 with $I > 10\sigma(I)$
Total recorded reflections	9740
Independent reflections (R_{int} (obs))	1383 (0.037)
Observed reflections ($I > 2.5\sigma(I)$)	688
Refinement results	
Refinement based on	F ($F(000) = 422$)
R/R_w (%) (all obs. ref. no.)	2.27/2.75 (688)
R/R_w (%) (all ref. no.)	5.06/2.88 (1383)
R/R_w (%) (main obs. ref. no.)	2.25/2.75 (676)
R/R_w (%) (1st satellite ob. ref. no.)	8.5/10.8 (12)
S (obs. ref.)	1.51
No. of refinement parameters	36
Weighting scheme	$w = 1/(\sigma^2\|F_o\| + (0.01\|F_o\|)^2)$
Residual electronic density, $e^-/Å^3$	[−3.24, + 3.08]

[a] $R = \sum \| F_o| - |F_c\| / \sum |F_o|$. $R_w = [w(|F_o| - |F_c|)^2 / \sum w|F_o|^2]^{1/2}$.

All the data reduction, absorption correction, Fourier, and refinement calculations were performed with the JANA98 program (18). The wave vector component was refined with the help of the U-FIT program (19) from main

reflections of both the H and Q parts. There is no satellite reflection satisfying the $I \geq 3\sigma(I)$ criterion in this data set. So, another data set corresponding to a larger exposure time (8 min.) was recorded using the same single crystal. In addition, a longer crystal-to-detector distance (100 mm) was set up to avoid overlapping effects. Unfortunately, only 12 satellite reflections have satisfied the $I \geq 2.5\sigma(I)$ criterion.

Starting from the structural model of $[((Pb,Fe)S)_{1.5}]_{1.15}NbS_2$, the atomic positions have been described in the superspace group $Cm2m(\alpha, 0, 0)$. In this homologue type, the Q part is a three-atom-thick layer (rock-salt type) with Pb atoms on the outer sides. First, only Mn-centered octahedron was considered, which led to a reliability factor $R = 4.27\%$ for 676 main reflections. The presence of residual peaks in the Fourier-difference map around the Mn site could indicate a Mn site split over four additional positions, the situation of which was therefore tested. In the same way, the S atoms coordinated to these Mn atoms were also statistically distributed over four positions. In addition, as the chemical analysis revealed a significant amount of niobium in the Q part, minor substitution of Mn by Nb, at the center of the octahedron, was tested with success (Fig. 3). All these considerations led to improve the R factor down to 2.66% for 27 variables. Finally, the displacive modulation waves were taken into account for atoms at the interface (i.e., S, Pb, and S1). The final R factor converged to 2.27% for all the 688 reflections and 36 variables (2.25% for the 676 main reflections and 8.5% for the 12 first-order satellites). The low improvement for the reliability factor means that the modulation of the atomic positions is very weak. All the refinement results are collected in Table 3. In this case the resulting structural formula $(Pb_{1.02}Mn_{0.39}Nb_{0.11}S_{1.50})_{1.15}NbS_2$ is found to be slightly different from that deduced by chemical analysis. However, by fixing the Nb/Mn substitution ratio to that corresponding to the chemical analysis, the structure refinement yields $R = 2.35\%$, which is very close to the previous result.

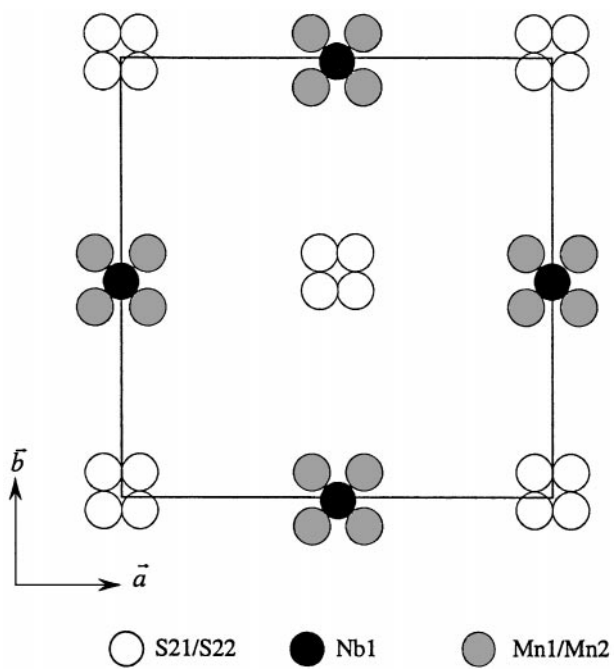

FIG. 3. Splitting of Mn and S atoms in the central layer of the Q part.

Structure Description

Figure 4 shows the arrangement of the two subsystems in the (b, c) plane of the whole structure along the incommensurate a direction. In the H part niobium atom is in a trigonal prismatic environment with quite identical Nb–S distances (2.48 Å). In the three-atom-thick Q layer, Pb atom, protruding at the margins, is coordinated by five S_Q atoms in a squared-pyramidal environment (Pb–S: ≈2.95 Å). In addition Pb atom is also bonded with S atoms of the H part (S_H). Figure 5 shows the modulated distances between Pb and S_H atoms with respect to the phase t. The minimum and maximum of the Pb–S_H bond lengths range from 3.03 to 3.98 Å (see the inset (a) in Fig. 5). The inset (b) shows the exchanged valences of this bonding according to the calculations detailed in the next part.

BOND VALENCE CALCULATIONS

The bond valence method (20, 21) was used to calculate the total bond valence at the interface of the two sublattices of the structure studied, and to make comparisons with some other misfit compounds. It is a semi-empirical method that relates the valence of each atomic bond to its length according to

$$v_{ij} = \exp[(R_{ij} - d_{ij})/b], \qquad [3]$$

where $b = 0.37$ is a universal constant, R_{ij} depends on the chemical nature of both elements, and d_{ij} is the interatomic distance of the (i, j) atom pair. A set of parameters R_{ij} has been deduced from a large number of known structures for several (i, j) couples of elements. It is known that Eq. (3) does not give a true measure of the bond valence in the case of a strained structure (22). However, that calculation has been already applied to misfit compounds (16, 23, 24). Clearly, geometrical constraints are occurring in this type of composite compounds because of mismatch and mutual interactions between both subparts. Our goal is to compare the strengths of the bonds at the interface of both subparts in various misfit compounds. Geometrical constraints effects are more or less of the same order in all these studied compounds, so that bond lengths that are correlated with bond valence could give comparative information, i.e., the

TABLE 3
Fractional Atomic Coordinates (a), Atomic Displacement (b), and Displacive Modulation Coefficients (c) for $(Pb(Mn,Nb)_{0.5}S_{1.5})_{1.15}NbS_2$

(a) Atom	v^a	Mult.	s.o.f.^{b}	x	y	z	U_{eq}
Nb	1	2b	1	0	− 0.0851(2)	0.5	0.0027(1)
S	1	4c	1	0	0.2481(3)	0.39114(8)	0.0064(3)
Pb	2	4a	1	0	0	0.20366(2)	0.01933(9)
S1	2	4e	1	0	0.4979(9)	0.1636(1)	0.0145(4)
Mn1	2	4e	0.195(3)	0.061(1)	0.432(3)	0	0.0125(9)
Mn2	2	4e	0.195(3)	0.061(1)	0.555(3)	0	0.0125(9)
Nb1	2	2a	0.22(1)	0	0.490(2)	0	0.005(2)
S21	2	4d	0.25	0.0417(5)	0.055(3)	0	0.012(1)
S22	2	4d	0.25	0.0417(5)	− 0.031(3)	0	0.012(1)

(b) Atom	U_{11}	U_{22}	U_{33}	U_{12}	U_{13}	U_{23}
Nb	0.0025(2)	0.0011(3)	0.0045(2)	0	0	0
Pb	0.0226(1)	0.0188(2)	0.0166(1)	0	0	− 0.0001(3)

(c) Atom (μ)	v	i	A_i^{μ}	B_i^{μ}
S	1	1	0.004(2)	0
S	1	2	0	− 0.0009(5)
S	1	3	0	− 0.0024(6)
Pb	2	1	0.0005(4)	0
Pb	2	2	0	− 0.0077(2)
Pb	2	3	0	0.0005(1)
S1	2	1	0.005(2)	0
S1	2	2	0	− 0.011(1)
S1	2	3	0	0.0007(7)

[a] $v = 1$, the atom belongs to the H subpart. $v = 2$, the atom belongs to the Q subpart.
[b] s.o.f.: the site occupancy factors of atoms are defined for each part independently. The weight ratio between these two parts is taken into account by the superspace structural description.

bond lengths depend on the charge transfer from the Q part to the H part. In other words, as the valence is a function of the interatomic distance, its value becomes a periodic function of t in incommensurate crystals (16).

The accuracy of bond valence calculations depends on the set of known crystal structures used to determine the R_{ij} parameters. It seems that the R_{ij}(Pb–S) value leads to a too high bond valence sum for Pb. Anyway, these calculations make possible comparisons between two structures involving the same chemical elements. The bond valence between M and X_H atoms was calculated for the compound studied together with some other misfit compound structures (Table 4). The valence excess (Ve) of the Q layer is calculated by multiplying the M–S_H bond valence by the weight ratio between the two parts $(1 + x)$. The bond valence sum of the cation T of the H part is deduced from the previous value using the following expression $(V - Ve)$, where V is the valence of T in the binary sulfide TS_2 and is equal to 4. In the case of the lacunary $(La_{0.94}[\ ]_{0.06}S)_{1.20}CrS_2$ compound (25), these calculations show that the average exchange valence between the lanthanum atom and the S atoms of the H sublattice (S_H) is 1 valence unit (v.u.) and only 2 v.u. with the S_Q atoms. This result agrees well with the expected value of an excess of one electron on the LaS sublattice. This is almost the same situation for $(LaS)_{1.14}NbS_2$. On the other hand, in the Pb compounds the exchange valence between the two sublattices is lower, as the oxidation state of Pb bound with S is strictly + 2. The amount of charge transfer is then restricted to cations with a valence above 2 in the Q part. For example the charge transfer is slightly higher in $(PbFe_{0.5}S_{1.5})_{1.15}NbS_2$ than in $(Pb_{1.0}Mn_{0.33}Nb_{0.16}S_{1.5})_{1.15}NbS_2$, due to the + 3 oxidation state of Fe, while the oxidation state of Mn bound with S is strictly + 2. The structural determination has shown (see above) that the Mn site is partially substituted by Nb (Nb(IV)?), which explains the excess of positive charge in the Q part.

CONCLUDING REMARKS

Charge transfer in misfit compounds with a (main) divalent M cation in the Q part was first proved on the basis

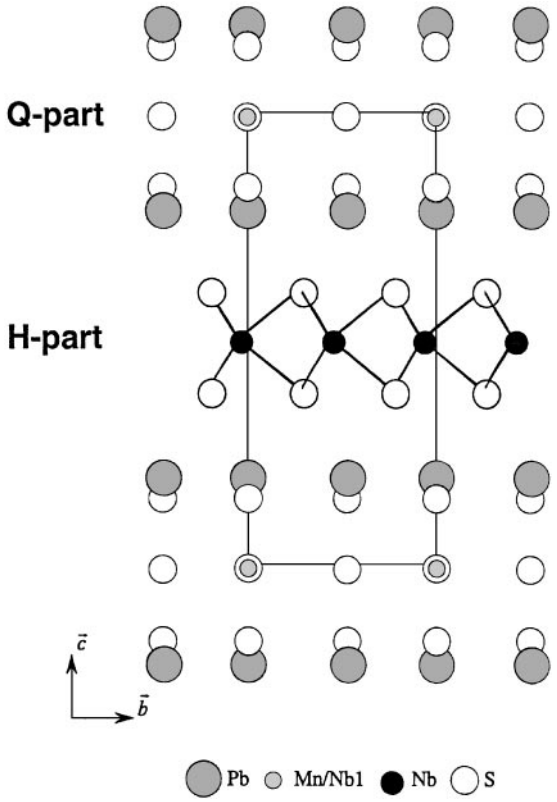

FIG. 4. Projection of the whole structure of $(Pb(Mn,Nb)_{0.5}S_{1.5})_{1.15}NbS_2$ along the incommensurate direction. For clarity, the splitted positions of Mn and S atoms belonging to the Q part have been omitted.

of chemical analysis for the 1Q/1H homologue $[(Pb,Nb)S]_{1.14}NbS_2$ (10), without confirmation through crystal structure (26) refinement. However, looking back to this structural study, the refined value (0.53) for the relative PbS/NbS_2 amount was found lower than the expected value (0.57) from the ratio of the *a* parameters. That tells in favor of a lesser Pb content and confirms, *a posteriori*, the partial substitution of Pb by Nb. In the new compound of the 1.5Q/1H type $(Pb(Mn,Nb)_{0.5}S_{1.5})_{1.15}NbS_2$, the incorporation of minor Nb within the Q layer, also indicated by electron microprobe analysis, is proved by an X-ray crystal structure determination through a superspace approach. The exact valence state of this minor Nb is difficult to assert, even through bond valence calculation, due to the splitting of S atomic positions in the central atomic plane of the Q layer. It could be approximated only indirectly from the valence excess of the Q layer. This valence excess is fully attributed to Nb, present in the Q layer, and therefore must be added to the $+2$ valences already exchanged with the S_Q atoms. This calculation leads to an oxidation state of about 4.5 which is overestimated due to the R_{ij}(Pb–S) value. According to Table 4, the oxidation state of Nb in the H layer varies from ~ 3 up to 3.6, which strongly determines the transport properties of Nb misfit compounds. In the title compound, this Nb oxidation state is close to that of the Mn-free 1Q/1H homologue, which is a superconductor. No such behavior down to 2 K was observed in the Pb/Mn phase, which

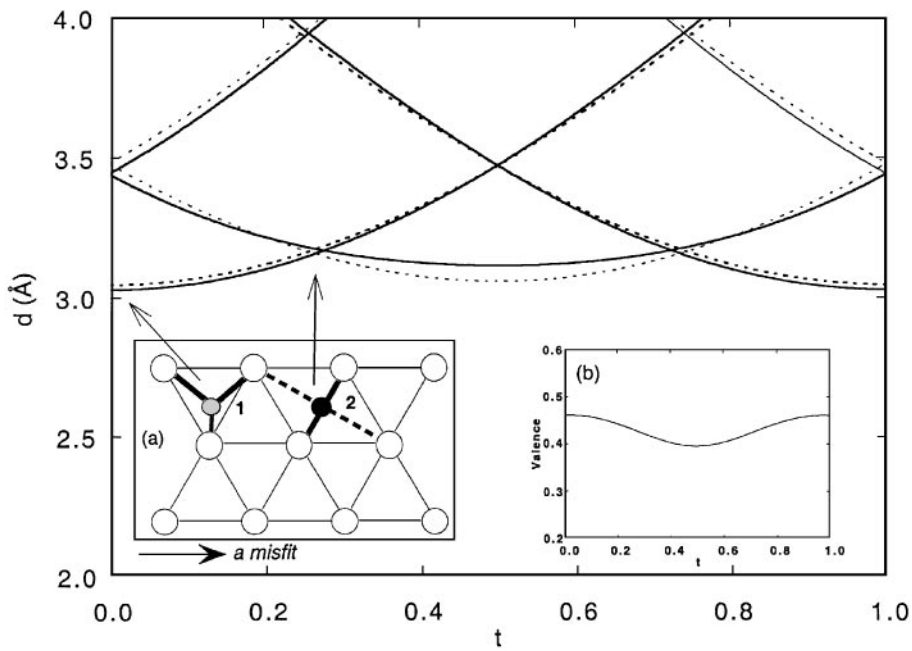

FIG. 5. Interatomic distances at the interface between Pb atoms (black and shaded circles) and S atoms (open circles) belonging to the H part of the misfit layered compound $(Pb(Mn, Nb)_{0.5}S_{1.5})_{1.15}NbS_2$. Basic-structure distances (dotted lines) are slightly different from modulated-structure distances (solid lines). The inset (a) represents the two cases: (1) corresponds to $t = 0$ with one distance of about 3 Å and two of about 3.45 Å; (2) corresponds to $t = 0.25$ with two short distances (≈ 3.15 Å) and two very long distances (≈ 4 Å). The inset (b) shows the exchange valence for this $Pb–S_H$ bond.

TABLE 4
Average Bond Valence for the Metal *M* Belonging to the Q Part with the S Atoms of the H Part (S_H) and with the S Atoms of the Q Part in Some Misfit Compounds $\{[(M, M')S]_m\}_{1+x}TS_2$

Compound	$d_{min}(M–S_H)$ (Å)	Ref.	R_{ij}[a] (for M–S)	Average bond valence sum $M \rightarrow S_Q$	Average bond valence sum $M \rightarrow S_H$	Valence excess of the Q layer (Ve)	T bond valence[c] (4 − Ve)
$(La_{0.94}[\ ]_{0.06}S)_{1.20}]CrS_2$(s.s.g.)	2.849	(27)	2.64	2.0	1.0	1.1	2.9
$(LaS)_{1.14}NbS_2$(c.a.)	2.883	(26)	2.64	2.15	0.9	1.05	~3[b]
$(Pb_{0.88}Nb_{0.12}S)_{1.14}NbS_2$(c.a.)	3.094	(10)	2.55	1.9	0.35	0.4	3.6
$(Pb_{1.0}Fe_{0.5}S_{1.5})_{1.15}NbS_2$(c.a.)	2.915	(8)	2.55	1.65	0.55	0.6	3.4
$(Pb_{1.0}Mn_{0.33}Nb_{0.16}S_{1.5})_{1.15}NbS_2$(s.s.g.)	3.027	This work	2.55	1.7	0.4	0.45	3.55
$[(EuS)_{1.5}]_{1.15}NbS_2$(s.s.g.)	2.873	(9)	2.53	1.35	0.6	0.7	3.3

Note. c.a., composite approach; s.s.g., in a superspace group.
[a] R_{ij} is the parameter used in the bond valence calculation according to the formula [3] in the text.
[b] The precise chemical analysis is not available.
[c] T = transition element in the H subpart.

is probably due to the presence of a magnetic cation (Mn^{2+}).

REFERENCES

1. G. A. Wiegers and A. Meerschaut, *in* "Incommensurate Sandwiched Layered Compounds" (A. Meerschaut, Ed.), Vol. 100 & 101, p. 101. Trans Tech, Zürich, 1992.
2. Y. Ohno, *Solid State Comm.* **79,** 1081 (1991).
3. A. R. H. F. Ettema and C. Haas, *J. Phys. Condens. Matter* **5,** 3817 (1993).
4. C. M. Fang, A. R. H. F. Ettema, C. Haas, G. A. Wiegers, H. van Leuken, and R. A. de Groot, *Phys. Rev. B* **52,** 2336 (1995).
5. A. Meerschaut, *Solid State Mater. Sci.* **1,** 250 (1996).
6. A. Meerschaut, Y. Moëlo, L. Cario, A. Lafond, and C. Deudon, *Mol. Cryst. Layered Cryst.* **341,** 805 (2000).
7. Y. Moëlo, A. Lafond, C. Deudon, N. Coulon, M. Lancin, and A. Meerschaut, *C.R. Acad. Sci. Paris* **325** (Sér. IIb), 287 (1997).
8. A. Lafond, C. Deudon, A. Meerschaut, P. Palvadeau, Y. Moëlo, and A. Briggs, *J. Solid State Chem.* **142,** 461 (1999).
9. L. Cario, A. Lafond, P. Palvadeau, C. Deudon, and A. Meerschaut, *J. Solid State Chem.* **147,** 58 (1999).
10. Y. Moëlo, A. Meerschaut, J. Rouxel, and C. Auriel, *Chem. Mater.* **7,** 1759 (1995).
11. A. Lafond, A. Nader, Y. Moëlo, A. Meerschaut, A. Briggs, S. Perrin, P. Monceau, and J. Rouxel, *J. Alloys Comp.* **261,** 114 (1997).
12. A. Janner and T. Janssen, *Acta Crystallogr. A* **46,** 408 (1980).
13. P. M. de Wolff, T. Janssen, and A. Janner, *Acta Crystallogr. A* **37,** 625 (1981).
14. V. Petricek, K. Maly, P. Coppens, X. Bu, I. Cisarova, and A. Frost-Jensen, *Acta Crystallogr. A* **47,** 210 (1991).
15. S. van Smaalen, *in* "Incommensurate Sandwiched Layered Compounds" (A. Meerschaut, Ed.), Vol. 100 & 101, p. 173. Trans Tech, Zürich, 1992.
16. S. van Smaalen, *Cryst. Rev.* **4,** 79 (1995).
17. STOE—IPDS Software, STOE & Cie (1996).
18. V. Petricek and M. Dusek, JANA98: Crystallographic computing system, Institute of Physics, Academy of Sciences of the Czech Republic (1998).
19. M. Evain, U-FIT: A Cell Parameter Refinement Program, *IMN-CNRS* (1992).
20. I. D. Brown and D. Altermatt, *Acta Crystallogr. B* **41,** 244 (1985).
21. N. E. Brese and M. O'Keefe, *Acta Crystallogr. B* **47,** 192 (1991).
22. I. D. Brown, *J. Solid State Chem.* **90,** 155 (1991).
23. P. Coppens, I. Cisarova, X. Bu, and P. Somme-Larsen, *J. Am. Chem. Soc.* **113,** 5087 (1991).
24. H. Leligny, D. Grebille, O. Pérez, A. C. Masset, M. Hervieu, and B. Raveau, *Acta Crystallogr. B* **56,** 173 (2000).
25. J. Rouxel, Y. Moëlo, A. Lafond, F. J. DiSalvo, A. Meerschaut, and R. Roesky, *Inorg. Chem.* **33,** 3358 (1994).
26. G. A. Wiegers, A. Meetsma, R. J. Haange, and A. Meerschaut, *Acta Crystallogr. B* **46,** 324 (1990).
27. V. K. Kato, *Acta Crystallogr. B* **46,** 39 (1990).